Preparation and Characterization of Poly(vinyl alcohol) Nanocomposites Made from Cellulose Nanofibers

E. H. Qua,[1] P. R. Hornsby,[1] H. S. S Sharma,[2] G. Lyons,[2] R. D. McCall[2]

[1]*Polymers Cluster, School of Mechanical and Aerospace Engineering, Queen's University Belfast, Ashby Building, Stranmillis Road, Belfast BT9 5AH, United Kingdom*
[2]*Applied Plant Science Division, Agri-Food and Bioscience Institute, Newforge Lane, Belfast BT9 5PX, United Kingdom*

Received 28 June 2008; accepted 25 January 2009
DOI 10.1002/app.30116
Published online 27 April 2009 in Wiley InterScience (www.interscience.wiley.com).

ABSTRACT: A method using a combination of ball milling, acid hydrolysis, and ultrasound was developed to obtain a high yield of cellulose nanofibers from flax fibers and microcrystalline cellulose (MCC). Poly(vinyl alcohol) (PVA) nanocomposites were prepared with these additives by a solution-casting technique. The cellulose nanofibers and nanocomposite films that were produced were characterized with Fourier transform infrared spectrometry, X-ray diffraction, thermogravimetric analysis, scanning electron microscopy, and transmission electron microscopy. Nanofibers derived from MCC were on average approximately 8 nm in diameter and 111 nm in length. The diameter of the cellulose nanofibers produced from flax fibers was approximately 9 nm, and the length was 141 nm. A significant enhancement of the thermal and mechanical properties was achieved with a small addition of cellulose nanofibers to the polymer matrix. Interestingly, the flax nanofibers had the same reinforcing effects as MCC nanofibers in the matrix. Dynamic mechanical analysis results indicated that the use of cellulose nanofibers (acid hydrolysis) induced a mechanical percolation phenomenon leading to outstanding and unusual mechanical properties through the formation of a rigid filler network in the PVA matrix. X-ray diffraction showed that there was no significant change in the crystallinity of the PVA matrix with the incorporation of cellulose nanofibers. © 2009 Wiley Periodicals, Inc. J Appl Polym Sci 113: 2238–2247, 2009

Key words: mechanical properties; nanocomposites; thermal properties

INTRODUCTION

There has been an increase in research activity on the preparation of polymer nanocomposites with cellulose nanofibers, which are known as cellulose microfibrils. Polymers reinforced with cellulose nanofibers are interesting because of the high aspect ratio and potentially excellent mechanical properties of cellulose nanofibers (modulus of ca. 150 GPa and tensile strength of ca. 10 GPa).[1] Cellulose nanocomposites may not only show major improvements in mechanical properties but also retain greater optical transparency with respect to other polymer composites.[2] In addition, there are abundant and renewable sources of cellulose matter from which microfibrils can be derived, including flax, hemp, kenaf, cotton, jute, wood, and sisal.

To enhance their compatibility with nonpolar polymers, cellulose nanofibers have been modified with using different approaches, including corona plasma discharge, coupling agent, surfactant and surface grafting, and derivatization methods. These approaches not only are difficult to carry out but also can adversely affect the reinforcing performance.[3–5] As a result, there is very limited literature available considering cellulose nanofibers in nonpolar and hydrophobic polymers, such as polypropylene and polyethylene.

The cellulose nanofibers used in this study were derived from flax fibers and microcrystalline cellulose (MCC). The major challenge envisaged in this study is the difficulty in isolating cellulose nanofibers aggregated from the parent feedstock. The potential applications of cellulose nanofibers are as thickeners in food products, as strengthening agents for packaging materials, as barrier coatings, and in lightweight and strong polymer nanocomposites.[6] To prepare stable suspensions, cellulose nanofibers have been prepared by sulfuric acid hydrolysis and suspended at a 1 wt % concentration. Sulfuric acid introduces negatively charged sulfate groups onto the whisker surface and results in the presence of electrostatic repulsion between the individual rigid cellulose nanocrystals.[7]

In this study, cellulose nanofibers were evaluated as reinforcing fillers for a water-soluble polymer, poly(vinyl alcohol) (PVA), which has hydrophilic properties and excellent film-forming ability. The hydrophilic property of this matrix was also likely to result in enhanced interfacial compatibility between the fibers and polymer matrix. The structure and mechanical properties of these nanocomposites were

Correspondence to: E. H. Qua (equa01@qub.ac.uk).

© 2009 Wiley Periodicals, Inc.

TABLE I
Process Conditions for the Preparation of Cellulose Nanofibers

Source	Sulfuric acid (wt %)[a]	Reaction temperature (°C)[a]	Reaction time (min)[a]	Acid/fiber pulp ratio[a]	Ball-milling process	Ultrasonic treatment
MCC	60	45	130	10	—	Yes
Flax	64	60	50	20	Yes	No

[a] Acid hydrolysis.

analyzed with Fourier transform infrared (FTIR), electron microscopy, X-ray diffraction (XRD), thermogravimetric analysis (TGA), dynamic mechanical analysis (DMA), and tensile property measurements.

EXPERIMENTAL

Materials

MCC (Asahi Kasei Chemicals Corp., Tokyo, Japan) and decorticated flax fibers (Linavabrik, Estonia) were chosen as the sources of nanofibers. PVA (P2 C20) was supplied by PVAXX, Ltd. (United Kingdom). As this is a proprietary development-grade material similar to C22, complete details of its formation, including its plasticizer content, are not available. However, it is a thermoplastic based on fully and partially hydrolyzed PVA combined with calcium carbonate, propylene glycol, and glycerol.[8]

Preparation of the nanofibers

Cellulose nanofibers generated from flax fibers and MCC were prepared with a combination of acid hydrolysis and ultrasonic techniques. Decorticated flax fibers were first manually cut to a length of 20–30 mm and then ball-milled at 600 rpm for 2 h. This was carried out with a planetary ball mill (PM100, Retsch, Leeds, United Kingdom). MCC and flax fibers were then hydrolyzed at 60°C for 50 min under the conditions shown in Table I. The mixture was centrifuged four or five times to remove the excess acid (10 min at 9500 rpm), and ultrasound (model 150T 150-W ultrasonic cleaner, VWR International, Leicestershire, UK) was applied for 30 min at 25°C. The supernatant was removed from sediments and replaced with distilled water to stop the hydrolysis reaction.

The centrifugation steps were repeated until the supernatant became turbid. This was then transferred into dialysis membrane tubes having a molecular weight cutoff of 8000 Da and dialyzed against tap water for 2 days until the pH of the suspension reached 7. The suspension was then passed through Whatman grade 41 quantitative filter paper to remove microparticles. The final concentration of the dilute suspension prepared was increased to 1 wt % with a Rotavapor (Bibby RE200, Sterillin Ltd., Burgoed, UK) at 40°C for approximately 1 h.

Preparation of the PVA film containing nanocellulose

To obtain a nanocellulose-reinforced PVA film, a 10 wt % aqueous solution of PVA powder was first prepared and stirred at 90°C for 1 h. The PVA solution was then mixed with a cellulose nanofiber suspension at a ratio of 95%/5% for another 30 min. The final suspension was then cast onto a Petri disc and dried at the ambient temperature for 5 days. The total dry weight of the composite film was approximately 5 g. The resulting composite film was then dried further in an oven at 70°C for 2 days before storage at 23°C and 50% relative humidity before characterization.

Electron microscopy

The size distribution of cellulose nanofibers was studied with a Philips transmission electron microscope (Philips M100 TEM, Philips, Eindhoven, The Netherlands) at an acceleration voltage of 100 kV. First, a droplet of a cellulose nanofiber suspension at a 1 wt % concentration was put onto a copper grid coated with a thin carbon film. To improve the contrast, the cellulose nanofibers were stained with a 1 wt % solution of uranyl acetate for 30 s. The sample was then dipped into a droplet of distilled water for 2 s to remove the excess uranyl acetate. It was then allowed to dry at the ambient temperature overnight.

Particle size measurements of cellulose nanofibers were undertaken according to the image analysis procedure described in ISO 13322-1:2004. To this end, dimensions of the cellulose nanofibers were determined from transmission electron micrographs with image analysis software (Jmicrovision 1.2.7, Jmicro Vision Co., Geneva, Switzerland). The number of selected particles was based on the particle size distribution and the desired confidence limits. From this analysis, the measurement of a minimum of 700 particles was required to achieve the mass-median diameter within a 30% error with 90% probability for nanoparticles having a maximum of 1.50 geometric standard deviations. The error with 90%

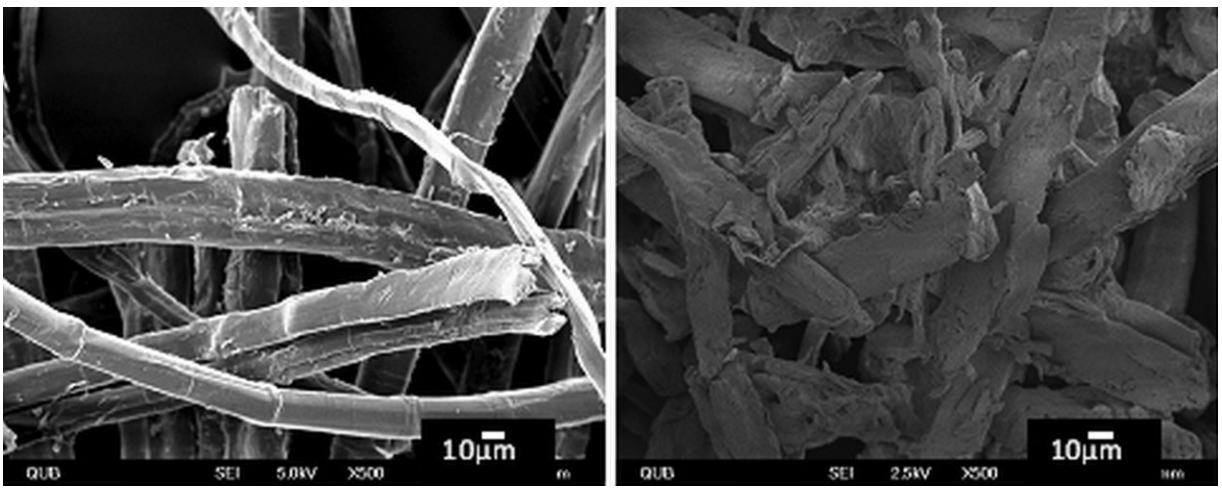

Figure 1 Scanning electron micrographs of the sources for cellulose nanofibers: flax fiber (left) and MCC (right).

probability for nanoparticles having a 1.45 geometric standard deviation would be 10% if based on the mean volume with the same number of particles. Wherever possible, touching particles were avoided to reduce measurement errors.

The morphology of the fracture surfaces of the composites was examined with a JEOL JSM-6500F scanning electron microscope (JEOL, Herts, UK). Samples were sectioned and sputter-coated with gold to prevent the buildup of an electrostatic charge.

FTIR analysis

FTIR spectra of the PVA film samples were obtained with a PerkinElmer Spectrum 1000 spectrometer (PerkinElmer Life and Analytical Sciences, Monza, Italy) equipped with a microscopic attachment (Autoimage system). The samples were cut to a thickness between 1 and 2 mm. The spectrum for each sample was recorded as an average of 64 scans at a resolution of 2 cm^{-1} in the range of 4000–500 cm^{-1} with a nitrogen-cooled detector.

X-ray analysis

XRD patterns from the cellulose nanocomposites were studied with an X'Pert Pro Panalytical X-ray diffractometer (Panalytical Ltd., Cambridge, UK) at 40 kV and 40 mA. The samples were scanned at the rate of 0.03 step/0.6 s with a Ni-filtered Cu Kα beam (wavelength = 1.5406 Å).

Thermal analysis

DMA

Dynamic mechanical thermal analysis (DMTA) of the PVA nanocomposites was undertaken in the tensile mode with a Triton DMA 2000 (Friedberg, Germany). The measurements were carried out at a constant frequency of 1 Hz with a 1 N preload, a strain amplitude of 0.1%, a temperature range of −30 to 100°C, a heating rate of 5°C/min, and a gap distance of 5 mm. The samples were prepared by the cutting of strips from the films with a diameter of 5 mm. Two types of films were prepared to examine the effect of water plasticization on the PVA films: (1) humidified films stored at 50% relative humidity (23°C) and (2) dried films conditioned at 55°C for 2 days before characterization.

TGA

The composite films were cut into small pieces (0.5–1 mm). Approximately 6-mg samples were tested with a microbalance and TGA unit (STA 851e with a TSO 80 RO sample robot, Mettler Toledo Ltd., Leicester, UK) at a heating rate of 20°C/min. The tests were carried out from 30 to 600°C in a nitrogen current of 50 mL/min. Derivative thermogravimetry (DTG) curves expressed the weight-loss rate as a function of time.

Mechanical properties

The tensile strength, modulus, and elongation at break were measured at 23°C with an Instron 4411 universal tensile testing machine (Instron, Bucks, UK) with a 2 kN load cell and a 50 mm/min crosshead speed according to ISO 527. At least 10 samples were taken from each specimen.

RESULTS AND DISCUSSION

Microscopy and appearance of the nanofiber composites

The original structure of the materials used in the investigation is shown in Figure 1, where it can be seen that the fiber dimensions are of the order of

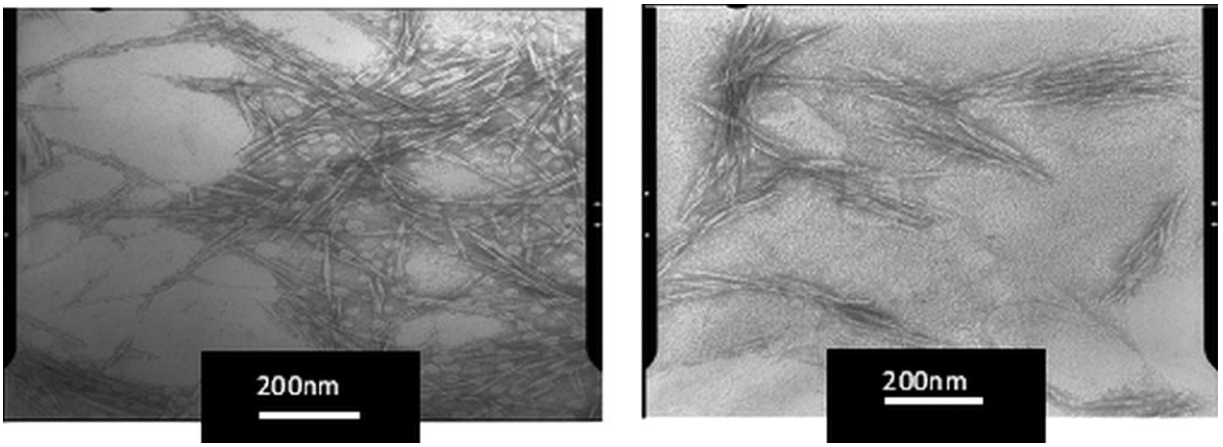

Figure 2 Transmission electron micrographs of cellulose nanofibers derived from flax fiber (left) and MCC (right).

micrometers. After acid hydrolysis and applied ultrasound, cellulose nanofibers were produced (Fig. 2). Size distributions for the length and diameter of the nanofibers obtained from MCC and flax are compared in Figure 3. From these results, MCC cellulose nanofibers were found to have lengths ranging from 21 to 300 nm and diameters ranging from 2 to 22 nm (Table II). The average values for the length and diameter were 111 ± 43 and 8 ± 2 nm, respectively. Cellulose nanofibers derived from flax fibers had lengths ranging from 21 to 350 nm and diameters ranging from 2 to 50 nm. The average length and diameter were estimated to be 9 ± 5 and 141 ± 57 nm, respectively. Therefore, the average aspect ratios (length/diameter) of the flax and MCC nanofibers were very similar, being approximately 17 and 14, respectively.

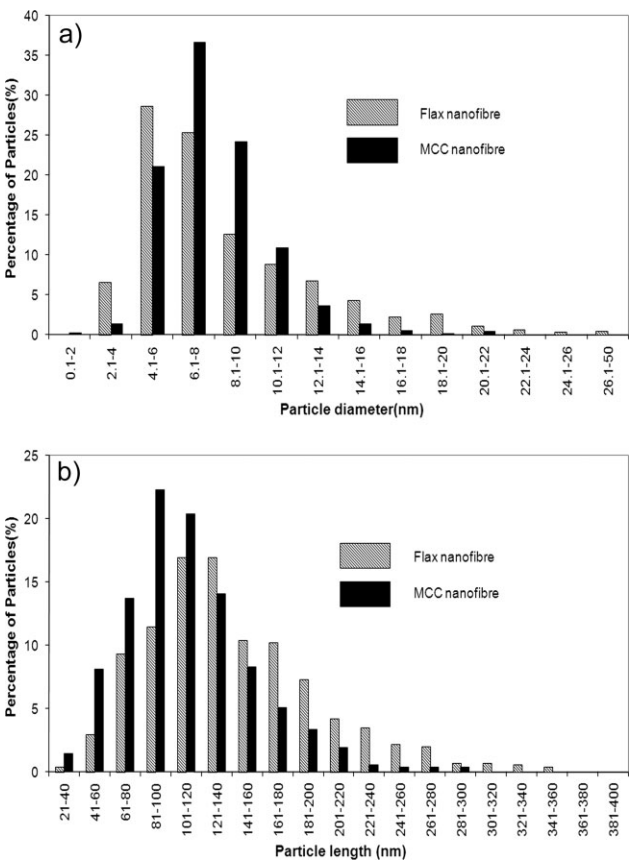

Figure 3 Size distribution of cellulose nanofibers: (a) diameter and (b) length.

Through casting from an aqueous solution, the PVA control gave a transparent, flexible film that was violet in color. The blends of PVA with MCC or flax nanofiber still showed flexibility and transparency. The presence of the residual organic materials, including lignin,[9] in the flax nanofiber made the PVA/flax nanofiber yellow-brown. The original color of MCC (white) altered the PVA matrix to pale violet.

The transparent nature of these nanocomposites (shown in Fig. 4) is a result of the cellulose nanofibers being far shorter than the wavelength of visible light. Cellulose nanofibers derived from flax fibers

TABLE II
Average Particle Sizes, Standard Deviations, Errors, and Axial Ratios of the Cellulose Nanofibers

		MCC nanofiber[a]	Flax nanofiber[a]
Diameter (nm)	Mean (nm)	7.9	8.5
	Standard deviation	2.4	4.5
Length (nm)	Mean (nm)	110.7	141.2
	Standard deviation	42.6	57.4
Aspect ratio (length/diameter)		14.0	16.6

The MCC nanofiber and flax nanofiber were cellulose nanofibers derived by acid hydrolysis from MCC and flax fibers, respectively, with a length between 20 and 30 mm.

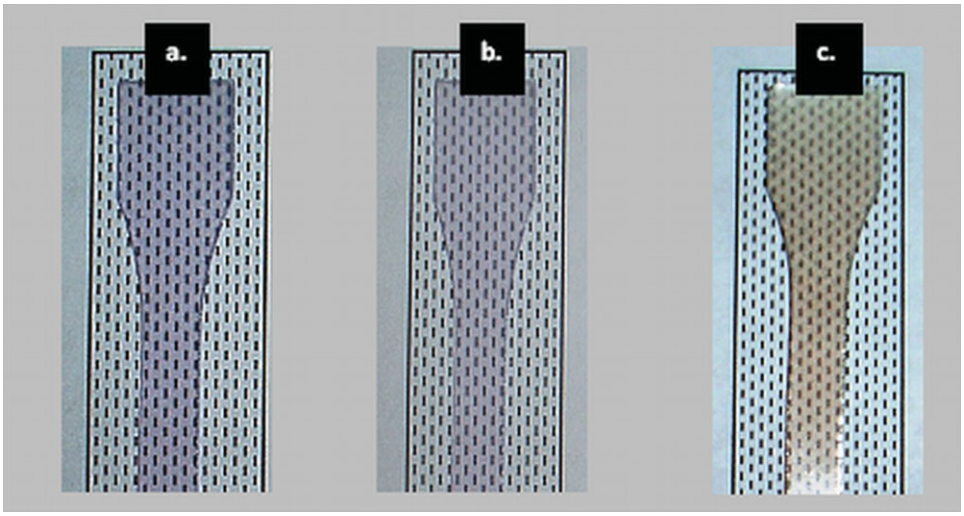

Figure 4 Appearance of the produced films: (a) PVA, (b) PVA/MCC nanofiber, and (c) PVA/flax nanofiber. [Color figure can be viewed in the online issue, which is available at www.interscience.wiley.com.]

and MCC appear as white dots on the fracture surface of the PVA nanocomposites (Fig. 5). This may indicate that there is very limited cellulose aggregation in PVA as a result of the high level of compatibility and interaction between the hydrophilic crystalline cellulose nanofibers and PVA matrix. However, the cellulose nanofibers (white dots) appear to be more prevalent for the PVA/flax nanofiber composition, and this may suggest that in the former system, the nanofibers are less well dispersed in the matrix.

FTIR analysis

Figure 6 shows FTIR spectra of the PVA, PVA/MCC nanofiber, and PVA/flax nanofiber films produced. The unmodified PVA film shows peaks at 3341 (—OH stretching), 2940 (alkyl CH stretching), 1715 (acetate C=O stretching), 1645 (H—O—H deformation), 1455 (CH bending), 1363 (CH bending), 1248 (acetate C—O bending), and 1092 cm^{-1} (C—O stretching). The presence of the peaks at 1715, 1363, and 1248 cm^{-1} can be attributed to the residual acetate groups in the PVA polymer.[10] The peak in the range of about 2230–2400 is omitted because the technique used is sensitive to carbon dioxide in the atmosphere.[11] The intensity of the broad band peak in the region of 1092 cm^{-1} increased with the addition of cellulose nanofibers to the PVA matrix because of the contribution of C—O stretching from the cellulosic component.

The addition of cellulose nanofibers to the PVA matrix has only a slight effect on the intensity of OH stretching. This may be due to the —OH groups on the surface of cellulose nanofibers interacting with adjacent —OH groups in the PVA without affecting the bonding between OH groups in the PVA matrix itself. The nature of the interface between the matrix and nanofibers is still unclear, and further work is needed to elucidate the role of the interaction in

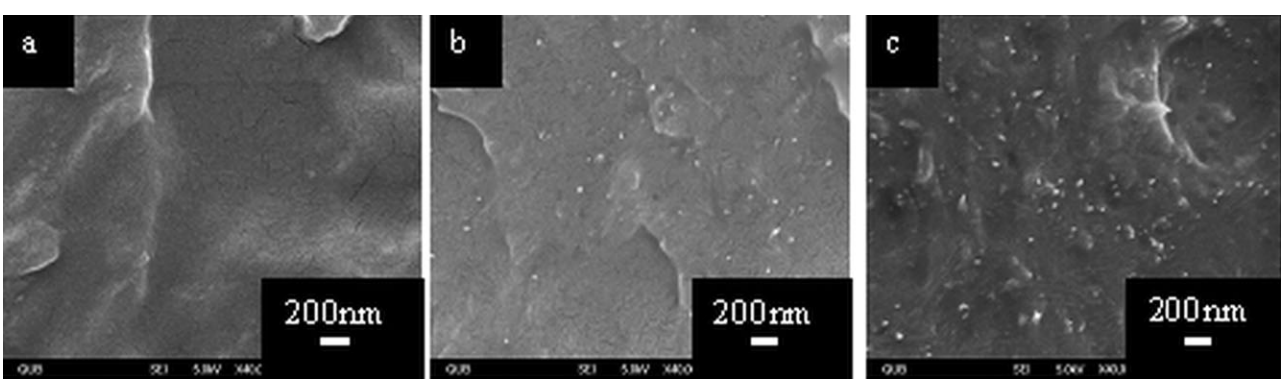

Figure 5 Scanning electron micrographs of the prepared PVA films: (a) PVA, (b) PVA/MCC nanofiber (5 wt %), and (c) PVA/flax nanofiber (5 wt %).

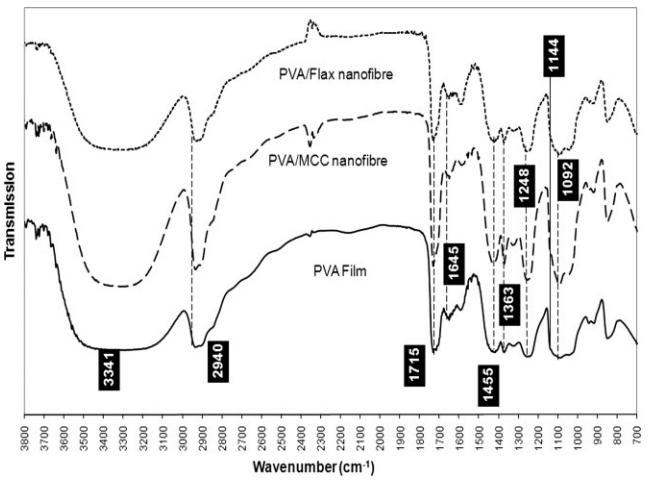

Figure 6 FTIR spectra of the produced films and cellulose nanofibers.

mechanical and thermal stability. However, FTIR results suggest that any interaction between the nanofiber and matrix is physical rather than chemical in origin.

XRD analysis

XRD diffractograms of the films produced and cellulose nanofiber powders are compared in Figure 7. The three main peaks at 2θ values of 14.9, 16.8, and 22.6° were observed in the curves for MCC nanofibers and flax nanofibers, corresponding to a cellulose I structure.[12] MCC nanofibers in this work were much less crystalline than flax nanofibers. This was apparently due to the low amorphous content of MCC and lack of a protective layer (lignin and hemicelluloses). Thus, the crystallites were first attacked during the hydrolysis, and this resulted in a decrease in the crystalline content.[13]

The PVA film showed a single scattering peak at 2θ = 19.5°, as reported previously.[14] The presence of a secondary peak at approximately 22.5° was observed in the PVA/MCC nanofibers and PVA/flax nanofiber films. This was obviously due to the contribution of the cellulose nanofiber included in the PVA composite. According to the reflection intensities of the PVA and PVA nanocomposites peak at 19.5°, the crystallinity of the PVA nanocomposite films was not significantly changed with a 5% weight addition of cellulose nanofibers. This lack of influence on the crystallinity is also supported by the FTIR absorption peak at 1144 cm^{-1} (C—O of doubly H-bonded OH in crystalline regions; see Fig. 6).[14,15]

Thermal analysis

DMTA results show the effects of temperature on the mechanical behavior, molecular relaxations, and interactions taking place in the PVA composites. The behavior of tan δ and the storage modulus for the composite products is shown in Figures 8 and 9. Table III presents the storage modulus at temperatures of −25, 30, and 70°C and the tan δ peak temperature.

As can be seen in Figures 8(a) and 9(a), the storage modulus of the two PVA composites, the PVA/MCC nanofiber and the PVA/flax nanofiber, increased over the entire temperature span in comparison with that of the PVA film. Figure 8(a) shows that the dried PVA composites showed only a slight increase in the storage modulus at 30°C in comparison with the unreinforced PVA film. At this temperature, there were only 9 and 21% improvements in the modulus for the PVA/MCC nanofiber and PVA/flax nanofiber, respectively, in comparison with the PVA film. However, at 70°C, the PVA composites showed significant increases in the storage modulus of 119 and 129% for the PVA/MCC nanofibers and PVA/flax nanofibers, respectively (see Table III). Meanwhile, the conditioned PVA composites (23°C and 50% relative humidity) showed a limited increase in their storage modulus at −25°C in comparison with the PVA film. However, these storage modulus improvements were much greater at higher temperatures (30 and 70°C). These results are illustrated and summarized in Figure 9(a) and Table III.

The glass-transition temperature (T_g) of the dried PVA film was approximately 35°C. However, the presence of cellulose nanofibers resulted in an increase of approximately 7°C for the PVA nanocomposites [Fig. 8(b)]. This arose from the restriction in segmental motion of the PVA molecules,[4] which was possibly influenced by a strong interaction between the PVA matrix and cellulose nanofibers.

The reduction in the tan δ peaks and significantly lower storage modulus values seen at 30°C when the samples were conditioned at 50% relative

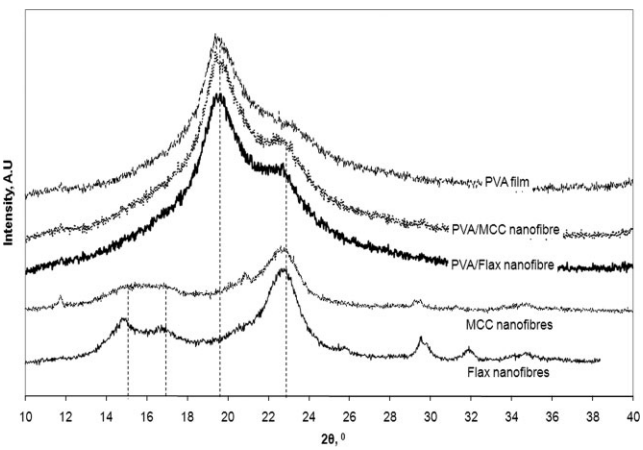

Figure 7 XRD patterns of PVA films.

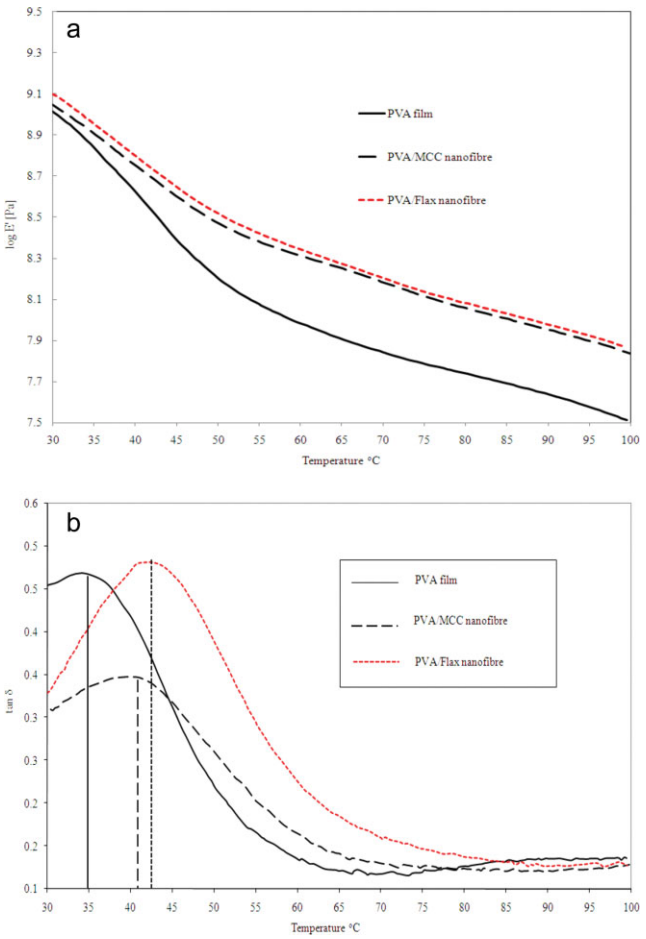

Figure 8 DMTA of PVA composites conditioned at 55°C: (a) storage modulus (E') curves and (b) tan δ peaks. [Color figure can be viewed in the online issue, which is available at www.interscience.wiley.com.]

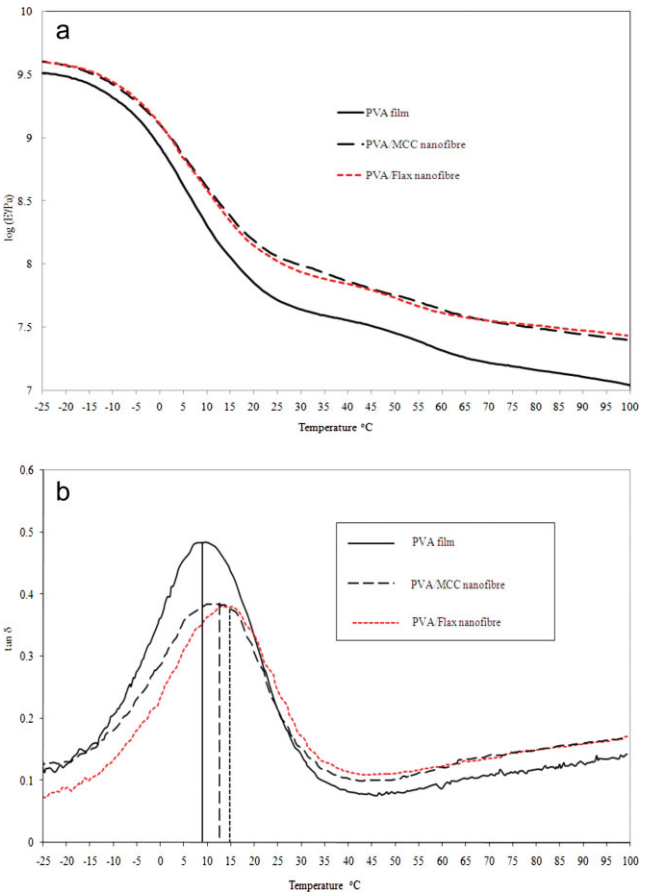

Figure 9 DMTA of the produced films (stored at 23°C and 50% relative humidity): (a) storage modulus (E') curves and (b) tan δ peaks. [Color figure can be viewed in the online issue, which is available at www.interscience.wiley.com.]

humidity and 23°C were due to plasticization of PVA (Fig. 9), demonstrating the moisture sensitivity of these materials due to the breaking of hydrogen bonds and the reduction of the cohesive energy between the polymer chains. Again, in these materials, both the storage modulus and tan δ of PVA increased when nanofibers were present.

Films containing cellulose nanofibers showed a slight increase in their storage modulus below T_g. This phenomenon is consistent with previously reported studies.[16–18] At temperatures below T_g, the matrix was glassy and rigid. Thus, there was no significant difference between the PVA control and PVA composites. Dufresne et al.[18] also reported that the difference between the elastic tensile modulus of cellulose nanofibers and that of the matrix is not high enough to benefit from a reinforcement effect in this temperature range. However, the PVA

TABLE III
DMA Results for PVA Nanocomposites Containing 5 wt % Cellulose Nanofibers

Condition	Material	Storage modulus (MPa)			Tan δ peak (°C)
		−25°C	30°C	70°C	
Stored at 55°C	PVA film	—	1030	70	35
	PVA/MCC nanofiber	—	1120	153	41
	PVA/flax nanofiber	—	1250	160	43
Stored at 23°C and 50% relative humidity	PVA film	3250	43	16	9
	PVA/MCC nanofiber	4020	98	34	13
	PVA/flax nanofiber	3960	82	35	15

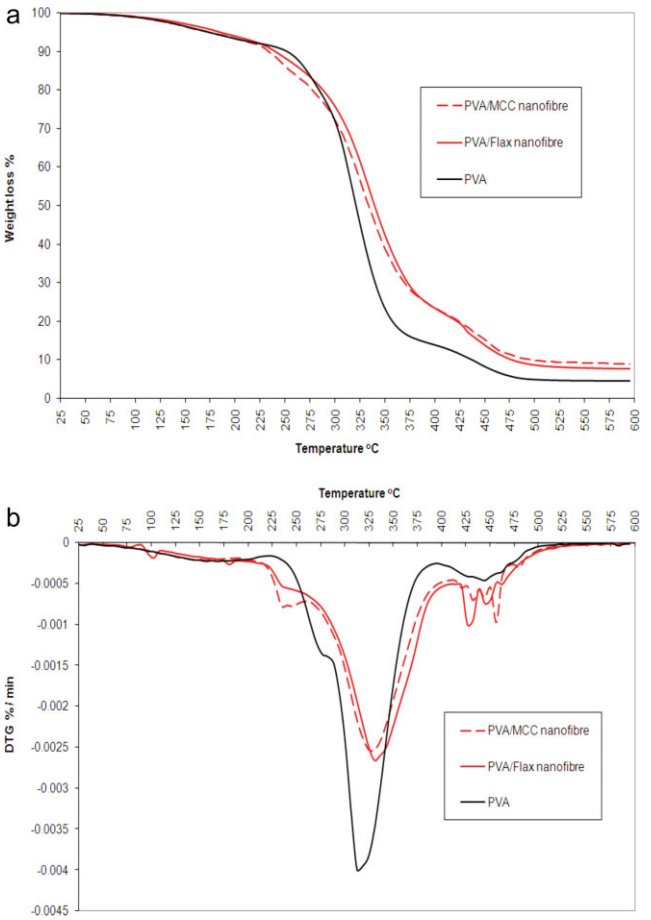

Figure 10 TGA curves under nitrogen for PVA nanocomposites: (a) thermogravimetric weight loss and (b) DTG curves. [Color figure can be viewed in the online issue, which is available at www.interscience.wiley.com.]

composites showed a significant improvement above T_g. Again, this is similar to previous studies.[16–18] This unusual reinforcing effect is in total contrast to the situation observed below T_g. This effect can be ascribed to the formation of a percolation network of cellulose nanofibers,[15] which results in the formation of a rigid cellulose nanofiber network within the PVA matrix above T_g, the cellulose nanofibers being linked through hydrogen bonds.[16]

TGA was undertaken in a nitrogen atmosphere to study the thermal stability of the materials produced. The presence of the three degradation steps for the produced films is evident from the weight changes in TGA and the derivatives of the weight-loss curves (Fig. 10). All the samples showed an initial weight loss around 75°C resulting from the loss of moisture in PVA upon heating.[9,19] The moisture contents in all the samples were similar, as shown in Table IV. It is evident that the weight loss of unreinforced PVA was close to that of the PVA nanocomposites before 217°C. After this point, the decomposition rate of the PVA nanocomposites showed a significant decrease in the presence of cellulose nanofibers, which reached a maximum lag at about 70°C. This was due to the restriction of the mobility of polymer chains and suppression of the decomposition as a result of the homogeneous distribution of cellulose nanofibers in the polymer.

Two main decomposition stages were observed in the DTG curve for a typical PVA film, and an additional decomposition stage was seen when cellulose nanofibers were present. The second and third degradation steps were consistent with the generally accepted mechanism for the degradation of PVA.[19,20]

Figure 10(b) shows that the second degradation peak of the PVA film was located at 307°C, and it increased significantly with the addition of cellulose nanofibers to the PVA matrix. The second degradation peaks at 335 and 329°C corresponded to the PVA/flax nanofiber and PVA/MCC nanofiber. The second stage of degradation mainly involves dehydration reactions and the formation of volatile products, as reported by Tsuchiya and Sumi[19,21] and Jia et al.[22] and as shown here:

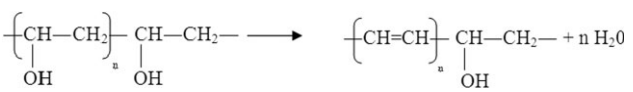

Because of the increased difficulty in breaking hydrogen bonds between the PVA matrix and cellulose nanofibers, the decomposition temperature in the second stage was increased when cellulose nanofibers were present.

The third degradation step corresponds to the degradation of polyene residues in the region of

TABLE IV
TGA Results for the PVA Films

Material	Moisture content (%)	Char at 500°C (%)	Onset temperature (°C)	T_{max} (°C) First stage	T_{max} (°C) Second stage	T_{max} (°C) Third stage
PVA	1.8	5.0	229	—	307	445
PVA/MCC nanofiber	1.9	9.9	219	237	329	435,463
PVA/flax nanofiber	1.5	8.7	217	236	335	430,450

T_{max}, peak temperature.

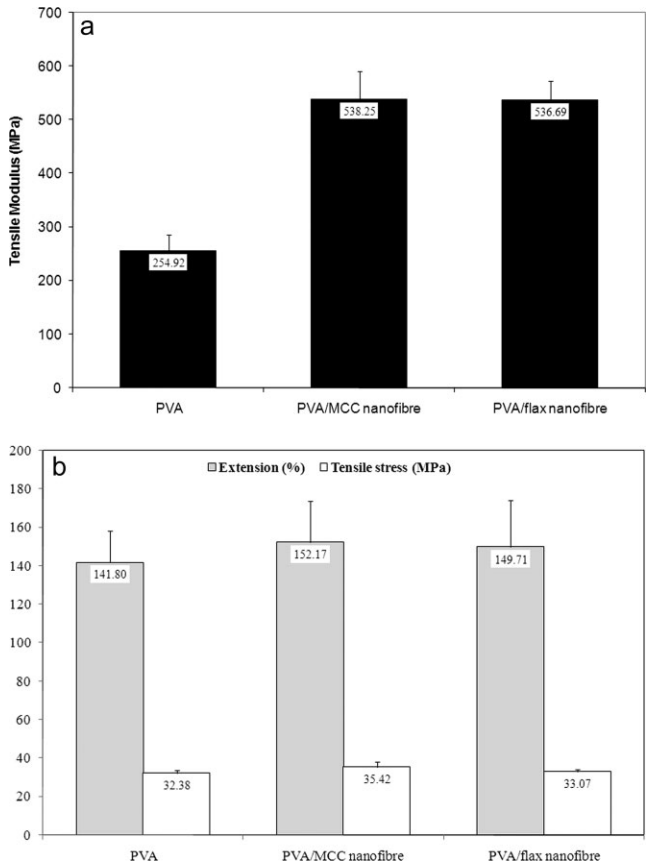

Figure 11 Mechanical property analysis of PVA films: (a) tensile modulus and (b) tensile stress and elongation.

450°C to yield a mixture of carbon and hydrocarbons, that is, *n*-alkanes, *n*-alkenes, and aromatic hydrocarbons.[21,22] In this stage, the decomposition temperatures of the cellulose nanocomposites and PVA film were similar. Another degradation peak, shown as a shoulder at 236°C, was observed in the PVA composites. This was apparently due to the presence of cellulose nanofibers and corresponded to the pyrolysis of cellulose nanofibers catalyzed by acid sulfate groups.[22–26] This resulted in the lower onset temperature of decomposition and the increasing amount of char residue at 500°C with the PVA composites in comparison with the PVA film. The onset temperature of the PVA film was 229°C, and those of the PVA composites were much lower than this, being only 219 and 217°C for the PVA/MCC nanofiber and PVA/flax nanofiber, respectively.

Mechanical properties

The tensile stress, modulus, and elongation to break of the nanocomposite PVA films are compared with those of unfilled PVA in Figure 11. The magnitude of the mechanical properties of the PVA films prepared in this study is significantly different from what has been previously published.[27,28] Typically, PVA shows tensile strength, modulus, and extension at break values of approximately 60 MPa, 2 GPa, and 100%, respectively.[27–29] There are several distinctions that may account for these differences. They are possibly due to the presence of the plasticizers, propylene glycol and glycerol, in the PVA matrix, which softened the PVA films with pronounced changes in the mechanical properties.[30] As mentioned previously, the PVA grade used in this study was a proprietary development grade believed to be different in composition from that used in previously published work, which did not contain a plasticizer.[27–29]

However, despite these differences in the properties of the base material, there was a 100% improvement in the tensile modulus of the PVA nanocomposites with the addition of cellulose nanofibers at only a 5 wt % concentration to the PVA matrix. This was attributable partly to the homogeneous distribution of cellulose nanofibers in the polymer, the inherent stiffness of the nanofibers, and the high level of compatibility between the fiber and matrix, which was aided by the high interfacial surface area. The hydrogen bonding between the cellulose nanofibers and PVA matrix resulted in the formation of a rigid network, yielding improved mechanical properties. However, the results for the PVA nanocomposites showed only a slight increase in the tensile stress and extension to break in comparison with the unmodified PVA matrix. Bhatnagar and Sain[28] studied the mechanical properties of PVA nanocomposites containing microfibrillated cellulose (10 wt %). They observed that the tensile strength showed a 10% improvement, whereas the tensile stiffness was 1.6 times greater in comparison with typical PVA. There are several distinctions that may account for these differences. First, in this work, cellulose nanofibers at only a 5 wt % concentration rather than at a 10 wt % concentration were added to the plasticized PVA. Second, different preparation methods were used to prepare the cellulose nanofibers. As a result, the microfibrillated cellulose was derived with a chemomechanical technique resulting in a longer fiber than that obtained in this work.

CONCLUSIONS

The structure and mechanical properties of PVA reinforced with cellulosic nanocomposites have been discussed. The objective of this investigation was to determine a methodology for the preparation of cellulose nanofibers for the reinforcement of PVA. To this end, cellulose nanofibers were successfully derived from flax fibers and MCC with a combination of acid hydrolysis and ultrasound. The addition of fibers (5 wt %) to PVA doubled the tensile modulus of the polymer and yielded optically transparent composites. Interestingly, the flax nanofibers showed the same relative reinforcing effects as MCC

nanofibers in the PVA matrix. This result was unexpected, and further work is required to verify this phenomenon. TGA results showed an apparent increase in the thermal stability of the composite with the presence of cellulose nanofibers. DMA results suggested that the use of cellulose nanofibers induced a mechanical percolation phenomenon leading to enhanced and unusual mechanical properties through the formation of a rigid filler network. FTIR and XRD results showed that the incorporation of cellulose nanofibers did not have an effect on the crystallinity of the PVA matrix. The use of cellulose nanofibers is limited to only laboratory-scale production (solution-casting process). To scale up to an industrial level, it is important to incorporate these cellulose nanofibers into polymers with commercial production techniques, in particular melt compounding. Improved cost-effective routes to preparing polymer compounds will be needed if large-scale use of cellulose nanofibers in commodity thermoplastics is to be achieved. This will require consideration of both extrusion and injection-molding processes and means for combining the fibers with polymer melts without degradation and agglomeration.

References

1. Oksman, K.; Mathew, A. P.; Bondeson, D.; Petersson, L.; Kvien, I.; Tanem, B. S. Processing of cellulose nanocomposites, 15–17 Sept, Hamburg, Germany. Proc Funct Fillers Plast 2004.
2. Nakagaito, A. N.; Yano, H. ACS Symp Series 2005, 938, 151.
3. Grunert, M.; Winter, W. T. J Polym Environ 2002, 10, 27.
4. Petersson, L.; Kvien, I.; Oksman, K. Compos Sci Technol 2007, 67, 2532.
5. Gopalan, N. K.; Dufresne, A.; Gandini, A.; Belgacem, M. N. Biomacromolecules 2003, 4, 1835.
6. Reitzer, R. Report: Technology Roadmap 2007: Applications of Nanotechnology in the Paper Industry; Nanoscience Center of the University of Jyväskylä: Jyväskylä, Finland, 2007.
7. Van den Berg, O.; Capadota, J. R.; Weder, C. Biomacromolecules 2007, 8, 1353.
8. PVAXX Technical Data Sheet; PVAXX R&D: Cirencester, United Kingdom, 2002.
9. Sen, S. K. Can J Chem 1963, 41, 2346.
10. Thomas, P. S.; Guerbois, J. P.; Russell, G. F.; Briscoe, B. J. J Therm Anal Calorim 2001, 64, 501.
11. Liao, W. T.; Lee, W.-J.; Chen, C. Y.; Hsieh, L. T.; Lai, C.-C. J Chem Technol Biotechnol 2000, 75, 817.
12. Mathew, A. P.; Chakraborty, A.; Oksman, K.; Sain, M. ACS Symp Series 2005, 938, 114.
13. Nisizawa, K. J Ferment Technol 1973, 51, 267.
14. Sriupayo, J.; Supaphol, P.; Blackwell, J.; Rujiravanit, R. Polymer 2005, 46, 5637.
15. Dunn, A. S. Polyvinyl Alcohol; Wiley: Chichester, England, 1992; Chapter 10.
16. Favier, V.; Canova, G. R.; Shrivastava, S. C.; Cavaille, J. Y. Polym Eng Sci 1997, 37, 1732.
17. Seydibeyoglu, M. O.; Oksman, K. Compos Sci Technol 2008, 68, 908.
18. Dufresne, A.; Kellerhals, M. B.; Witholt, B. Macromolecules 1999, 32, 7396.
19. Tsuchiya, Y.; Sumi, K. J Polym Sci Part A-1: Polym Chem 1969, 7, 3151.
20. Maruyama, K.; Takeuchi, K.; Tanizaki, Y. Polymer 1989, 30, 476.
21. Tubbs, R. K.; Wu, T. K. Polyvinyl Alcohol; Wiley: New York, 1973; Chapter 8, p 167.
22. Jia, X.; Li, Y.; Cheng, Q.; Zhang, S.; Zhang, B. Eur Polym J 2007, 43, 1123.
23. Wang, N.; Ding, E.; Cheng, R. Polymer 2007, 48, 3486.
24. Kim, D. Y.; Nishiyama, Y.; Wada, M.; Kuga, S. Cellulose 2001, 8, 29.
25. Julien, S.; Chornet, E.; Overend, R. P. J Anal Appl Pyrolysis 1993, 27, 25.
26. Staggs, J. E. J. Polymer 2006, 47, 897.
27. Wang, B.; Sain, M. ACS Symp Series 2005, 938, 187.
28. Bhatnagar, A.; Sain, M. J Reinforced Plast Compos 2005, 24, 1212.
29. Paralikar, S. M.S. Thesis, Oregon State University, 2007.
30. Toyoshima, K. Properties of Polyvinyl Alcohol Films; Wiley: 1973; Chapter 13, p 331.